



# Development, validation and application of a newly developed rig facility for investigation of jet aeroacoustics

Leopoldo Pacheco Bastos<sup>1</sup> · Cesar J. Deschamps<sup>2</sup> · Andrey R. da Silva<sup>2</sup> · Julio A. Cordioli<sup>2</sup> · José R. L. N. Sirotto<sup>2</sup> · Igor A. Maia<sup>2</sup> · Eduardo L. C. Coelho<sup>3</sup> · Rudner L. Queiroz<sup>3</sup>

Received: 26 December 2016 / Accepted: 25 November 2017  
© The Brazilian Society of Mechanical Sciences and Engineering 2018

## Abstract

Over the last decades, significant improvements have been achieved in terms of noise reduction for jet engine aircraft. Nevertheless, jet noise remains one of the major sound sources from commercial aircraft, particularly during take-off. To develop strategies for jet noise reduction, it becomes paramount to understand the mechanisms of sound production and radiation from the experimental point of view. For this reason, researchers need high-quality noise data, obtained under proper conditions for both the acoustic and flow fields of scaled jets. This paper reports the development, validation and application of a new jet rig facility built at Federal University of Santa Catarina for investigations of jet noise. Issues relating to limited budget, deadline fulfillment and inner space restrictions, made the design and construction of the facility particularly difficult. Such drawbacks were overcome by designing carefully every system making up the whole facility, some of them based on CFD analyses, as well as by employing tailored solutions to some systems. Throughout the paper, the infrastructure of facility and its main systems are presented as well as major design requirements are discussed. Subsequently, the free-field qualification and the determination of acoustic far-field for the jet source, concerning the anechoic chamber, are described. With the aim of evaluating the acoustic performance of the facility, noise data were acquired for jet flows with Mach numbers from 0.3 to 0.9 and observer locations from 60 to 150 degrees. Additionally, hot-wire anemometry measurements were performed at different axial positions along the jet to illustrate the turbulent character of flows generated. Results of flow and noise measurements revealed an acoustically clean signature as well as turbulence properties in good agreement with data from other facilities. Finally, the paper outlines the underway research works at the mentioned facility and new directions for further work.

**Keywords** Rig facility · Jet noise · Scaled jets · Anechoic chamber

## 1 Introduction

Aircraft noise is associated with major environmental issues, including noise pollution [1, 2], and several adverse effects to human health such as sleep disruption, increases in blood pressure [2] and, in extreme cases, hearing impairment [3]. According to Barbot et al. [4], aircraft

noise is one of the main causes of nuisance and loss of quality of life, particularly for those who live and work within airport areas. As a result, the policies and protocols related to admissible acoustic emissions and noise certification of aircraft have become more stringent over the last decades [5, 6].

One of the major sources of aircraft noise is still the noise produced by the engine jet, particularly during take-off [1, 7]. Numerical and experimental approaches have been successfully employed to investigate jet noise and flow fields produced by the engine [8–13]. Computational tools have proven to be very useful for predicting jet noise with simplified configurations [8–10]. However, for more complex jet flows the computational approach implies high computational costs, given the high-order numerical schemes necessary for the calculations of both acoustical

---

Technical Editor: André Cavalieri.

---

✉ Leopoldo Pacheco Bastos  
leopbastos@ufpa.br

<sup>1</sup> Federal University of Pará-CAMTUC, Tucuruí, PA, Brazil

<sup>2</sup> Federal University of Santa Catarina, Florianópolis, SC, Brazil

<sup>3</sup> EMBRAER, São José dos Campos, SP, Brazil

and fluid fields [14, 15]. Thus, the experimental approach is an obvious alternative to assess the main mechanisms associated with generation and propagation of sound from jets. Hence, it becomes paramount to build jet rig facilities, where both the acoustic and flow fields of scaled jets can be adequately reproduced and investigated [16–18].

A jet rig is designed to reproduce all the acoustic conditions required for the investigations of aerodynamically generated sounds, particularly those produced by jets [16–20]. In short, the facility must be able to provide: (1) a free-field acoustic environment; (2) dry air; (3) high Reynolds number flows; and (4) turbulence intensity levels representative of full-scale applications [19, 21]. Moreover, it is highly recommended that the facility has low background noise levels and a relatively low cutoff frequency for the free-field condition [21, 22]. If these requirements are met, the jet rig becomes a very important tool, not only for understanding fundamental phenomena associated with aerodynamically generated sound but also to propose specific strategies for aircraft noise mitigation [1, 23]. In this context, the use of jet rigs has provided valuable information and assisted the aviation industry to develop new technologies [24–29].

The aim of this paper is to provide a thorough discussion of major requirements to design a jet rig facility. This is accomplished by describing the development, validation and subsequent use of a newly developed jet rig at Federal University of Santa Catarina (UFSC), Brazil.

The paper is organized as follows. Section 2 provides a general description of the facility including its main components and characteristics. Still, in Sect. 2, some difficulties encountered in original project are discussed and the solutions applied to overcome them are presented. Section 3 discusses the requirements for accurate results from the acoustic point of view and describes the acoustic characterization of the jet rig chamber according to the ISO 3745 standard. The methodology adopted to assess the acoustic far field of the jet-generated sound is presented in Sect. 4, along with the procedure used to establish noise data repeatability. Section 5 presents the comparison between noise results generated by different subsonic flow conditions and those provided by the literature for the same operation characteristics. Finally, Sect. 6 underlines the fundamental aspects when designing a jet rig and their importance for carrying out research on aeroacoustics.

## 2 Facility description

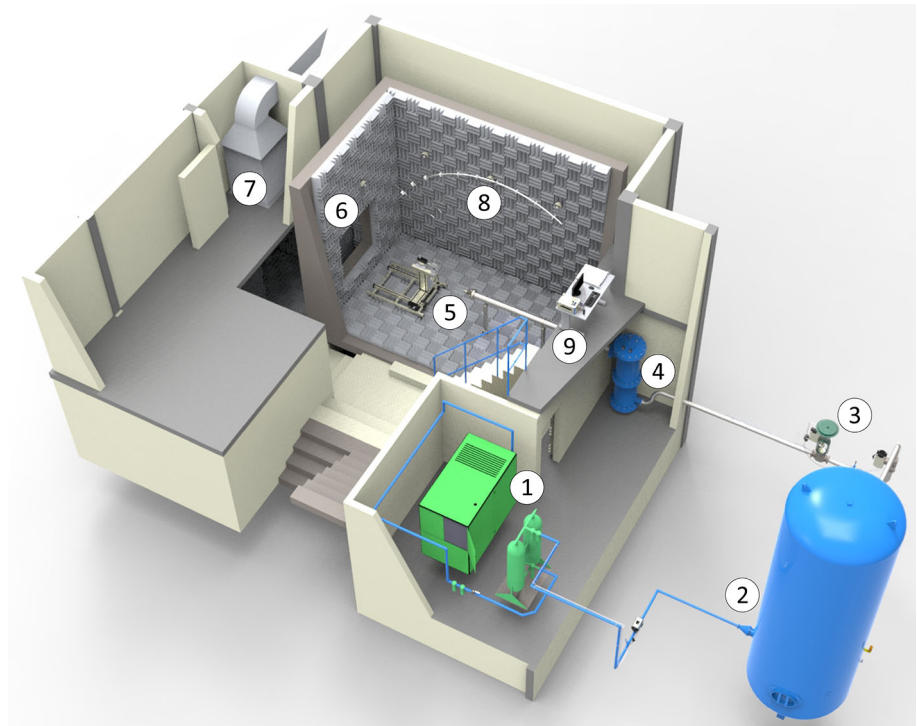
The rig developed at the Federal University of Santa Catarina [30], depicted in Fig. 1, is the first facility in Latin America for the investigation of jet aeroacoustics, and it was initially designed to perform tests with cold-scaled jets

at high subsonic speeds. The facility is composed by an air conditioning unit, consisting of a compressor, a heatless air dryer and a filter unit (item 1) connected to a 15 m<sup>3</sup> air reservoir, from which the air flow is discharged (item 2). This air flow is controlled by an automated system composed of block and control valves (item 3) to avoid pressure fluctuations and allow for the interruption of the air supply for safety reasons. Before reaching the test environment, the air flow passes through a plenum (item 4), allowing the reduction of noise from upstream line due to flow unsteadiness. Moreover, the plenum was designed to keep the internal flow velocities low and to provide large area contractions between the plenum and the test section to minimize turbulence at the exit plan. The stagnation properties of the air inside the plenum are used to calculate the acoustic Mach number of the jet based on the isentropic flow condition described further. Inside the test chamber (item 5), the flow line terminates in a 6-in. flange that allows for the connection of different nozzles. A jet collector (item 6), designed with the aid of Computational Fluid Dynamic (CFD) simulations, located in the opposite side to the nozzle, assists in the removal of air discharged inside the test chamber, whereas an acoustic muffler (item 7) acts to attenuate the noise levels before leaving the test environment. The noise is acquired from a microphone array (item 8) positioned in the acoustic far field. All facility operations are executed using an integrated control system based on the LabView software, which is operated on the same PC used to perform the acoustic measurements. The hardware is placed in a control room adjoining to the test chamber (item 9). This integrated control system allows for controlling remotely the air conditioning unit as well as monitoring and registering the test environment parameters such as temperature, total pressure and humidity.

### 2.1 Test chamber and acoustic lining

According to Ahuja [19], the test chamber must be large enough to comply with acoustic far field condition, microphone positioning and measurement angle requirements. All of them are correlated with each other by means of the model nozzle scale or test nozzle diameter ( $D_j$ ), which is one of the most important design parameters since it defines the noise frequency spectrum for typical experiments. The frequency range of the jet noise of modern engines, with a nozzle diameter of approximately 0.5 m, usually goes from 20 Hz to 10 kHz [19]. The comparison between results obtained with a scaled nozzle and real engines is made possible using a model-to-engine scale factor. This is usually performed by considering the Strouhal number,  $fD_j/U_j$ , where  $f$  is the frequency (Hz) and  $U_j$  is the jet velocity. This allows the noise data obtained

**Fig. 1** Jet rig facility at the Federal University of Santa Catarina: 1—conditioning unit; 2—air reservoir; 3—block and control valves; 4—plenum; 5—test chamber; 6—jet collector; 7—acoustic muffler; 8—microphone array; 9—control room



from the experiments with the scaled nozzle to be extrapolated to full-scale jet engine applications [19]. Based on the expected frequency range, one can select the acoustic lining (in terms of dimensions and sound absorption characteristics) as well as the data acquisition system and transducers.

Additionally, the test nozzle diameter is also considered when defining the dimensions of other important components of the facility, such as the air supply system, the jet collector, among others. The product of the maximum jet velocity (m/s) to be investigated, the test nozzle area (m<sup>2</sup>) and the air density (kg/m<sup>3</sup>) determines the maximum mass flow rate (kg/s) required for the experiments. From this parameter, the air reservoir volume can be specified, followed by the compressor mass flow rate and the filtering capacities of the heatless dryer. Additionally, from the maximum jet velocity, one can estimate the jet plume size and then the required dimensions for the jet collector on the opposite side to the nozzle, based on the jet spreading angle. Of course, small facilities with significant inner space limitations must be designed to use efficiently the available space.

The aforementioned test environment requirements are more easily met in larger facilities, but the cost of building these facilities is very high [21]. Besides, additional difficulties related to maintenance and deadline for the construction were mandatory for turning an existing reverberant chamber into a fully anechoic test chamber. The test chamber used in this facility has a 0.28-m-thick

wall, made of reinforced concrete structure, which provides high sound insulation to the test environment, so that the background noise does not interfere with the experiments. The measurements are carried out in a 60 m<sup>3</sup> fully anechoic room built inside a structurally disconnected external room to minimize the transmission of noise and vibration from the external environment.

The initial investigations at UFSC's jet rig facility have been carried out for a 2-in. test nozzle diameter (around 1:10 scale relative to a full-scale engine nozzle), implying that the expected frequency range for typical experiments should go from 200 Hz to 100 kHz [19], according to the Strouhal number relation. To comply with the anechoic behavior requirement for this frequency range and to overcome the inner space limitations, a tailored acoustic lining was designed (Fig. 2). The lining was made of 0.2-m-deep melamine foam with good resistance to mold, microbial growth and provides low flame spread in the case of fire. The wedges were installed on alternated arrangements of three horizontal by three vertical units, providing a cutoff frequency at around 400 Hz (more details in Sect. 3). The inner effective dimensions of the anechoic chamber are 5 m length, 4.05 m height and 2.95 m width, measured from the tips of the lining wedges.

## 2.2 Air supply system and plenum

An indispensable requirement to conduct investigations of jet noise is to supply good quality air for the experiments.



**Fig. 2** Test chamber interior and details of acoustic wedge arrangement

This implies the delivery of dry air in a steady manner [19]. For facilities that operate with compressor and storage tank, it is also important that the air supply system allows sufficiently long measuring windows. This is a crucial requirement when investigating flow field characteristics using point-by-point measuring devices (such as hot-wire anemometers, for example), which is usually a lengthy process. The reservoir loading time should be also considered when designing the air supply system to keep the facility's idleness down.

To avoid those problems, some facilities employ a predicated compressor, which operates continuously without the need of storage tanks. Nevertheless, such equipment is normally large and expensive, the reason why it has not been chosen as a solution for the UFSC's jet rig facility. Alternatively, the jet rig at UFSC uses the air from a reservoir with maximum operating pressure of 12.5 bar. The air is pressurized into the reservoir by a compact oil-free single-stage screw compressor at a maximum volume flow rate of  $0.175 \text{ m}^3/\text{s}$ . The reservoir loading time normally takes about 25 min from completely empty condition to working pressure condition, providing measuring

windows that last nearly 30 min for jets of Mach 0.5. The air supply system, depicted in Fig. 3, also controls the air humidity, eliminates the presence of solid particles, and supplies steady dry air at controlled temperature and pressure.

As previously mentioned, the plenum is an element of the airline with two main objectives: (1) reduce the noise from the upstream line, and (2) provide a stagnation point, which is a resetting point of the flow condition and allows the calculation of nozzle exit Mach number,  $M$ , by means of the isentropic flow equations. The flow equation used is based on relation of pressures given by

$$\frac{P_0}{P} = \left[ 1 + \left( \frac{\gamma - 1}{2} \right) M^2 \right]^{\frac{\gamma}{\gamma - 1}}, \quad (1)$$

where  $P_0$  is the stagnation pressure measured in the plenum,  $P$  is the static pressure inside the test chamber, and  $\gamma$  is the ratio of specific ratios assumed to be 1.4 for air.

### 2.3 Jet collector and entrainment air

The test environment of a jet rig facility is supposed to simulate the main characteristics associated with free-field operation [19]. This includes reproducing adequately the mechanism of jet entrainment and the absence of acoustic reflections, at least within the frequency range of interest. High-speed jets normally entrain a large quantity of ambient air as part of the thrust generation process [31]. Therefore, for every anechoic chamber to work properly as a jet rig facility, it is important to allow the free entry (entrainment) of air into the chamber as well as to provide adequate means of exhausting the discharged air [16, 19, 32]. This is usually achieved by making air inlet and outlet (jet collector) vents in the test chamber. Obviously, the vents must be made wisely not to compromise drastically the sound insulation of the chamber and to prevent noise pollution to the outer environment. Additionally, these vents are also intended to keep a constant pressure in the chamber and to avoid recirculation zones [32].

Providing the correct conditions for adequate air entrainment in small facilities is particularly challenging due to the reduced inner space [16]. Moreover, there are no general rules to accurately design air inlets and outlets. Therefore, numerical simulations were carried out with the CFD++ software to assess the resulting flow field for different inlet and outlet geometries as well as vent locations inside the test chamber. The result of a typical simulation is depicted in Fig. 4, in which the influence of inflow vents on the aerodynamic behavior of a 0.9 Mach jet flow is shown in a streamline plot. Based on the CFD results, it was found that a 0.8-m square acoustically

**Fig. 3** Air supply system of UFSC’s jet rig facility

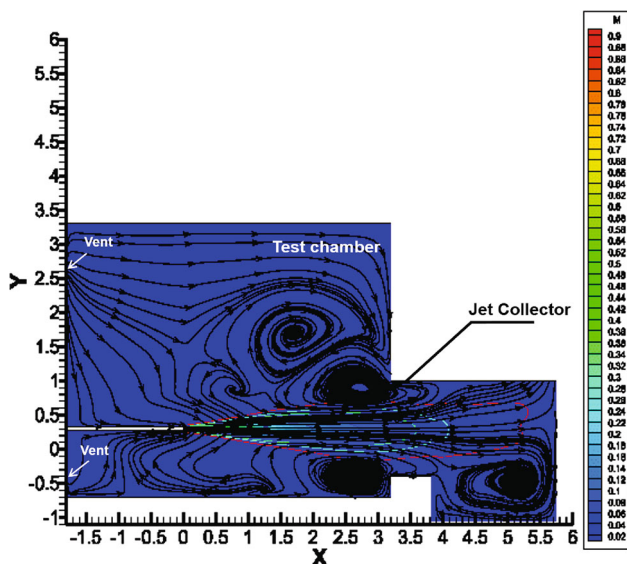
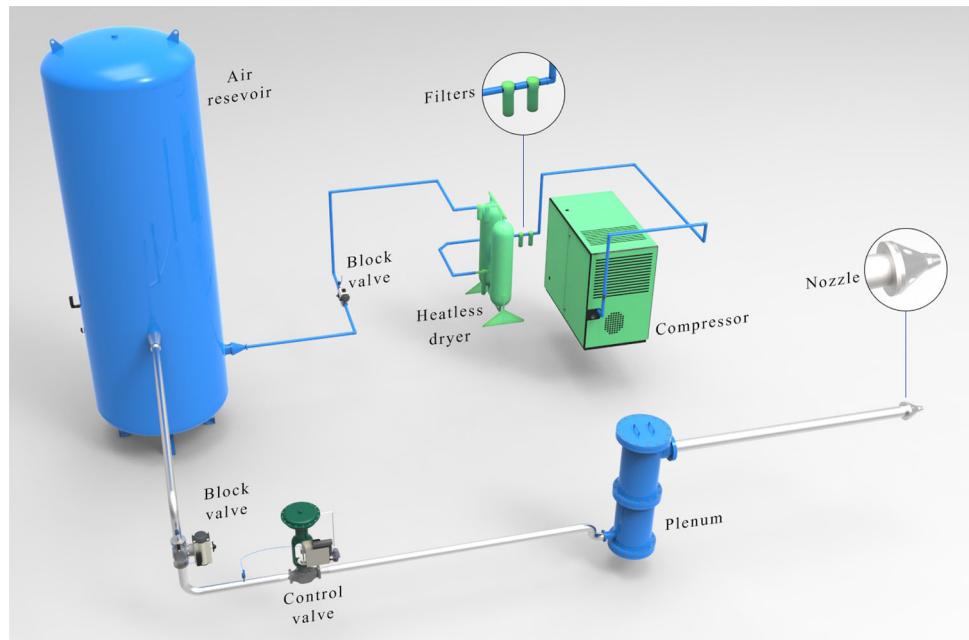


**Fig. 4** Simulation result of a 0.9 Mach cold jet inside the test chamber: streamlines and jet plume characteristics

treated air inlet and a 1.4-m square jet collector in the opposite side sufficiently meet the flow field requirements. The jet collector was designed mainly based on the spreading characteristics of tested jets whereas the air inlet was dimensioned to keep the velocity of air flow as low as possible near the microphones and to avoid recirculation zones.

### 2.4 Data acquisition system and microphone array

The noise data are acquired using 10 free-field 1/4" microphones, model GRAS 46BE-S1, distributed along an arc-shaped array positioned in the polar axis relative to the nozzle (Fig. 5), from 60° to 150° at 10° intervals, where 180° corresponds to the nozzle exhaust flow direction. Noise data acquisition is conducted with an NI PXIe-1082 eight-slot chassis (National Instruments), having maximum sampling rate of 204.8 kS/s per channel, and using specific software designed in LabView.

The flow measurements are performed with a hot-wire anemometry system (Dantec Dynamics) consisting of an automated arm and one-dimensional anemometer probes

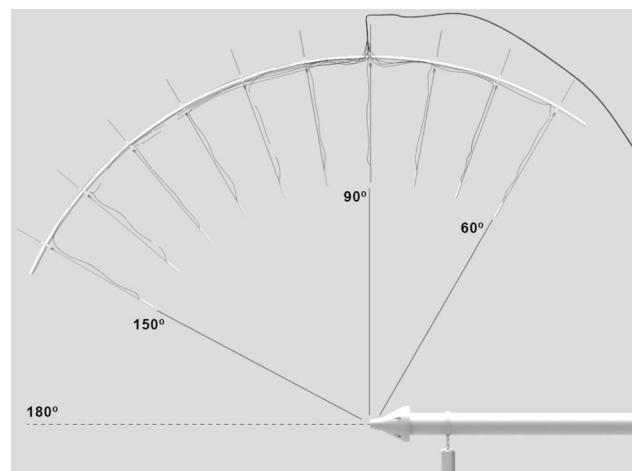


**Fig. 5** Positioning of the arc-shaped array relative to the nozzle

with miniature wires of 5  $\mu\text{m}$  diameter and 1.25 mm length, recommended for working in high-speed flows (up to 500 m/s) and temperatures (up to 150  $^{\circ}\text{C}$ ). In the present work, tests were performed using 2-in. (0.0508 m)-diameter nozzles, originally investigated by Bridges and Brown [33], namely SMC 000 and SMC 006 (Fig. 6).

To attain good stability during the experiments, a control loop was implemented on the integrated control system to adjust the control valve opening as a function of the thermodynamic variables measured inside the plenum and the test chamber. These variables serve as input for the isentropic flow equation described previously. The flow data are acquired by the integrated control system at each 0.1 s thus allowing a near real-time adjustment as well as providing steady flows after an initial transient regime, which varies from 10 to 15 s, depending on the operating condition (Fig. 7). The solid lines in Fig. 7 represent the reference values corresponding to the nominal velocities. It has been observed variations on jet velocity of less than 2% (6 m/s) for Mach 0.5 and even smaller for higher velocities.

### 3 Acoustic validation

#### 3.1 Data acquisition system (DAQ)

This section intends on analyzing the data acquisition system, looking to identify the frequency range in which the system frequency response can be considered flat, and where the measurements would have acceptable errors due to the DAQ. The methodology consists of generating a white noise in the same spectral frequency used by the data acquisition and analyzing the frequency response of the DAQ [13]. A PXI-6726 card and a connector block SCB-68A, both from NI, were connected to the PXIe system and



**Fig. 6** Geometry of nozzles tested: SMC 000 (on left) and SMC 006 (on right)

used to generate a 1 V amplitude white noise. The signal was fed to the DAQ, which acquired data for 20 s with a 120 kHz sampling frequency. Figure 8 displays the measured data analyzed in 50 Hz narrow band in blue and a software-fitted curve in red. Without the oscillations found in the measured data, the fitted curve is used for analysis.

The DAQ response has a flat region with deviations lower than 0.3 dB up until the 55 kHz frequency. Higher deviations above 55 kHz can be found, with values as high as 4 dB in 60 kHz. Distortions up to 0.3 dB are accepted. For precaution, it was chosen not to acquire data higher than 50 kHz in narrow band, thus the 1/3 octave band will extend until the 40 kHz nominal frequency.

#### 3.2 Free-field qualification of test chamber

The most important function of a fully anechoic test chamber is to reproduce accurately free-field conditions. To achieve this, the chamber must absorb almost completely the acoustic energy incident on the wedges at the frequency range of interest. From lower to higher frequencies, the frequency at which the energy absorption exceeds 99% is generally known as the cutoff frequency.

To determine the anechoic properties of the test chamber, ISO 3745 standard [34] was used, which provides all procedures demanded to the free-field qualification. A 13-in.-diameter (0.33 m) dodecahedral sound source which complies with the requirements regarding omnidirectionality, source compactness, high-output sound levels and stability required by ISO 3745 standard was used. Regarding the chamber, the main requirement of ISO 3745 standard establishes that sound pressure levels (SPL) recorded must decay 6 dB with doubling of the distance to the source (inverse square law) within the following tolerances for three different frequency ranges:  $\pm 1.5$  dB below 630 Hz,  $\pm 1.0$  dB from 800 to 5000 Hz and  $\pm 1.5$  dB above 6300 Hz. These tolerances must be fulfilled at any location more than a quarter wavelength away from the wedges and from a distance of 0.5 m from the sound source.

The dodecahedral source was placed on a tripod positioned at the geometric center of the chamber, as depicted in Fig. 9, and then, SPL measurements were conducted from 0.6 to 1.4 m away from the source center, by 0.1 m increments, towards different directions, numbered from 1 to 5. A Bruel & Kjaer PULSE analyzer was used to send a pink noise input signal to the dodecahedral source over a frequency range from 100 Hz to 12.5 kHz in one-third octave bands for 15 s measuring windows. To register the SPL in each point, the acquisition system and the microphones described in the previous section with similar signal processing settings were used. The SPL values referring to all directions are also shown in Fig. 9, in which the solid

**Fig. 7** Velocity curves for jets from different operating conditions during a control stability test

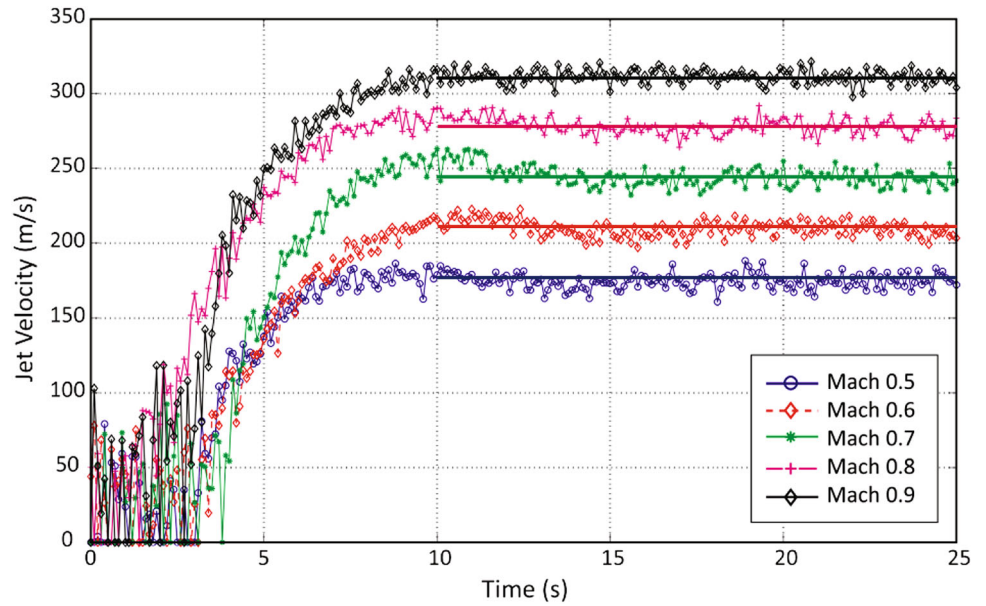
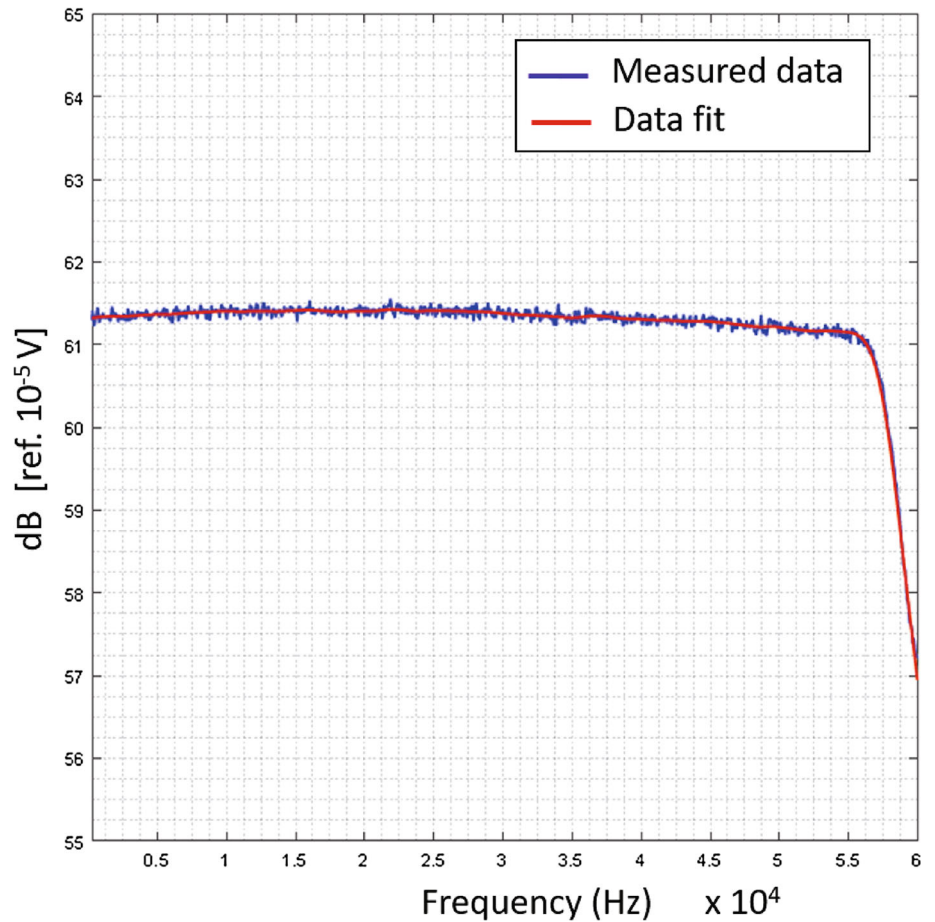


**Fig. 8** DAQ frequency response function for 120 kHz sampling frequency and the fitted curve



black lines correspond to SPL measured as a function of distance to the source, whereas the dashed red lines refer to theoretical decay of the sound levels. One can observe that for 100 and 250 Hz, the SPL does not decay in a monotonic

linear fashion within the range of measured distances, which indicates that the far-field condition cannot be reached for these frequencies. This behavior is due to the low absorption capability of the acoustic treatment at this

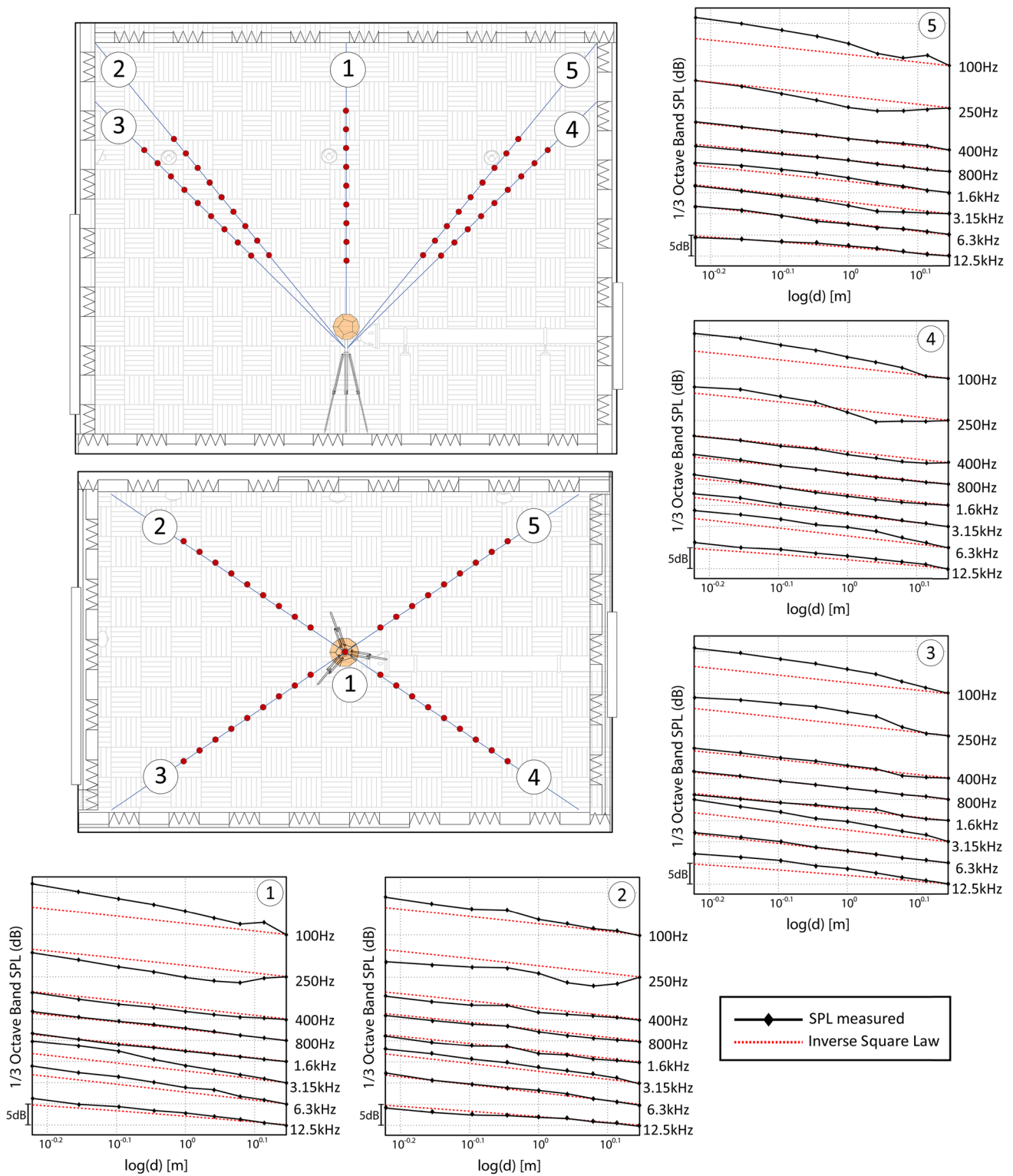


**Fig. 9** Free-field calibrations and schematics of positioning of dodecahedral sound source and microphones during the anechoic chamber qualification

frequency range. For 400 Hz, a more consistent monotonic behavior is observed and the sound pressure levels present a linear decay with the distance, respecting the tolerances

for every measurement point. This behavior is even more stable for 800 Hz and this trend is kept for higher frequencies. For 1.6 and 3.15 kHz it is possible to observe a

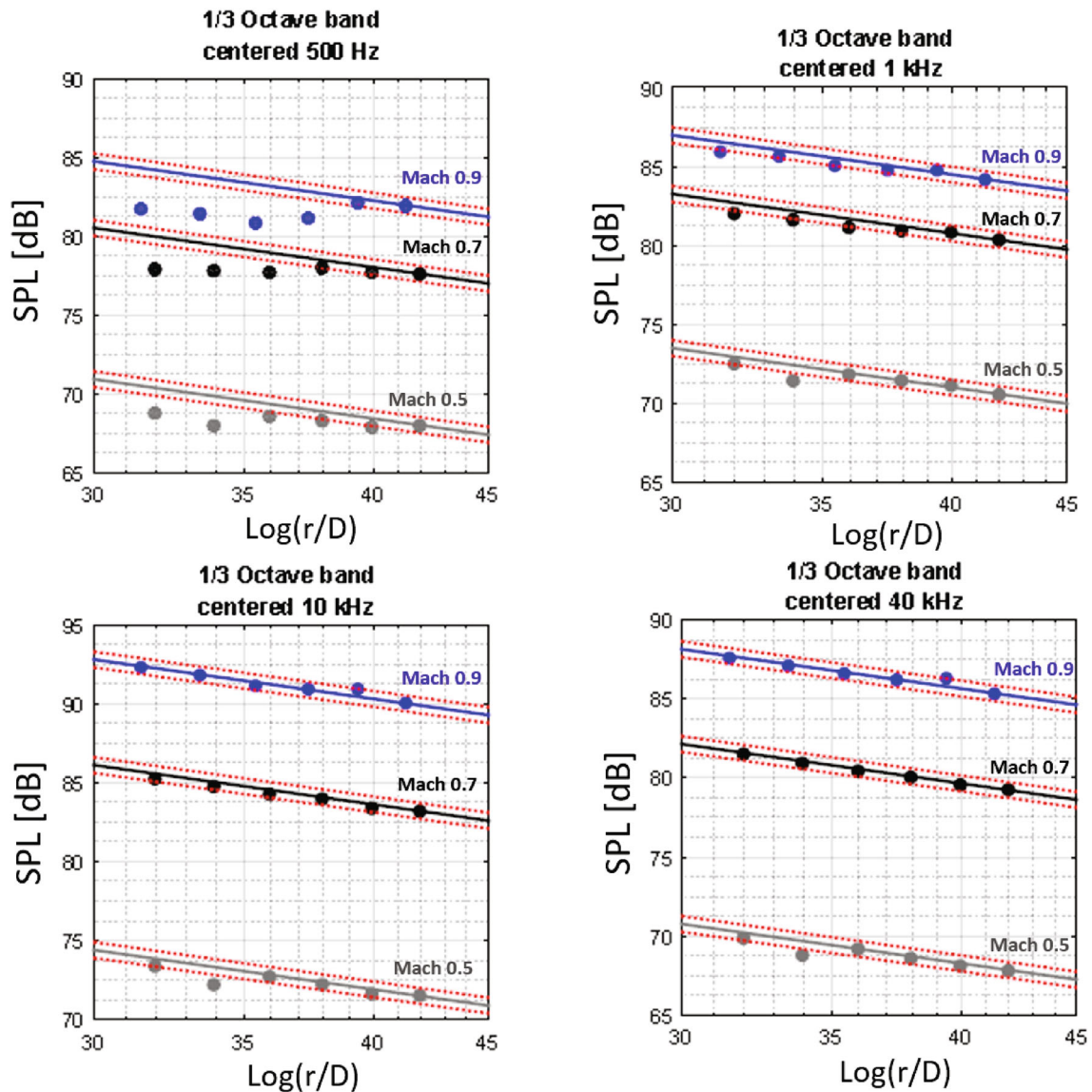


**Fig. 10** Far-field law for different frequencies from the SPL data in 1/3 octave bands for varying radial distances and Mach numbers from 0.5 to 0.9, issued by SMC000 and microphone location of 90°

slight non-linear behavior. Nevertheless, this is not associated with a near-field condition but rather, with the high directivity pattern of the dodecahedral sound source at frequencies above 1 kHz. Thus, 400 Hz was established as cutoff frequency for direction 2.

Similar behavior is observed for the other microphones and their cutoff frequencies are as follows: 315 Hz for direction 1, 315 Hz for direction 3, 315 Hz for direction 4 and 315 Hz for direction 5. Therefore, based on the results for all directions, the cutoff frequency of the test chamber was established as 400 Hz.

### 3.3 Acoustic far-field test for the jet source

To determine the radial extension of the region in which the inverse square law is valid for the jet source, a similar test conducted for free-field qualification was carried out. The difference is that the jet was used as a point source instead of a compact sound source. A similar procedure was also used by Ahuja and Jansson [16, 19]. The analysis used four angular positions (60°, 90°, 120° and 150°) and six radial distances from the nozzle center, ranging from 32 to 42 Dm, for a 2" (0.0508 m) diameter nozzle (SMC000).

Measurements were repeated five times for each Mach condition, namely Mach 0.5 (gray points), 0.7 (black points) and 0.9 (blue points), considering the microphone location of 90°, and are presented in Fig. 10. In addition, an

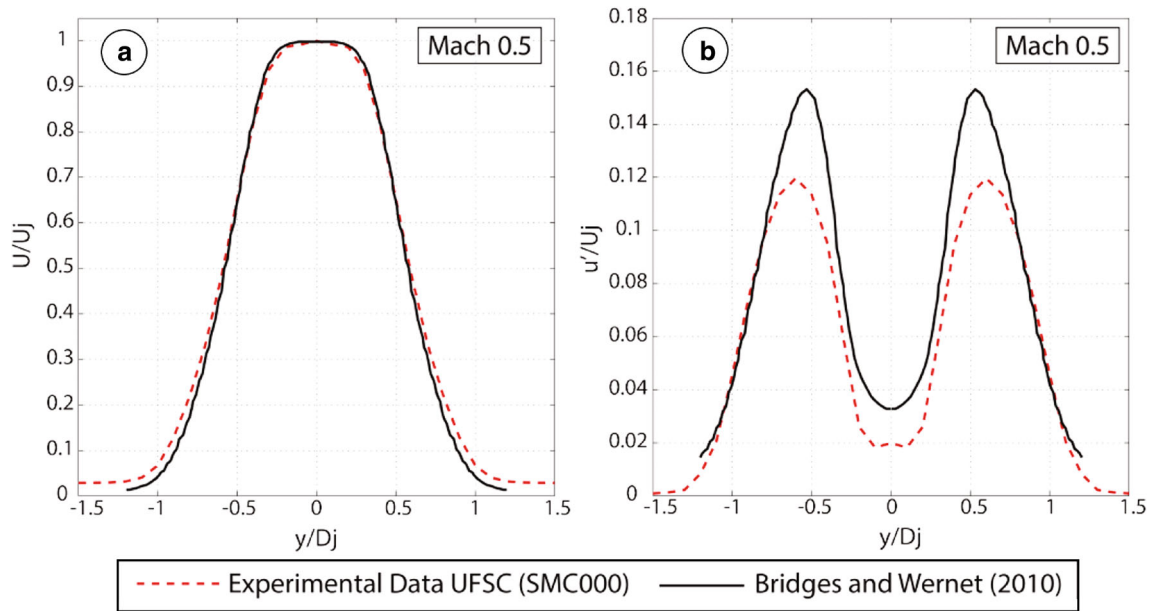


**Fig. 11** Comparisons of **a** velocity and **b** turbulence intensity profiles: experimental results from the present work and data from Bridges and Wernet [37] at  $x/D_j = 4$ ; Mach 0.5 and nozzle SMC 000

**Fig. 12** Acoustic data repeatability for the  $150^\circ$  microphone location, concerning five different test campaigns using SMC 000 nozzle and 0.5 Mach jets. Data obtained at narrowband

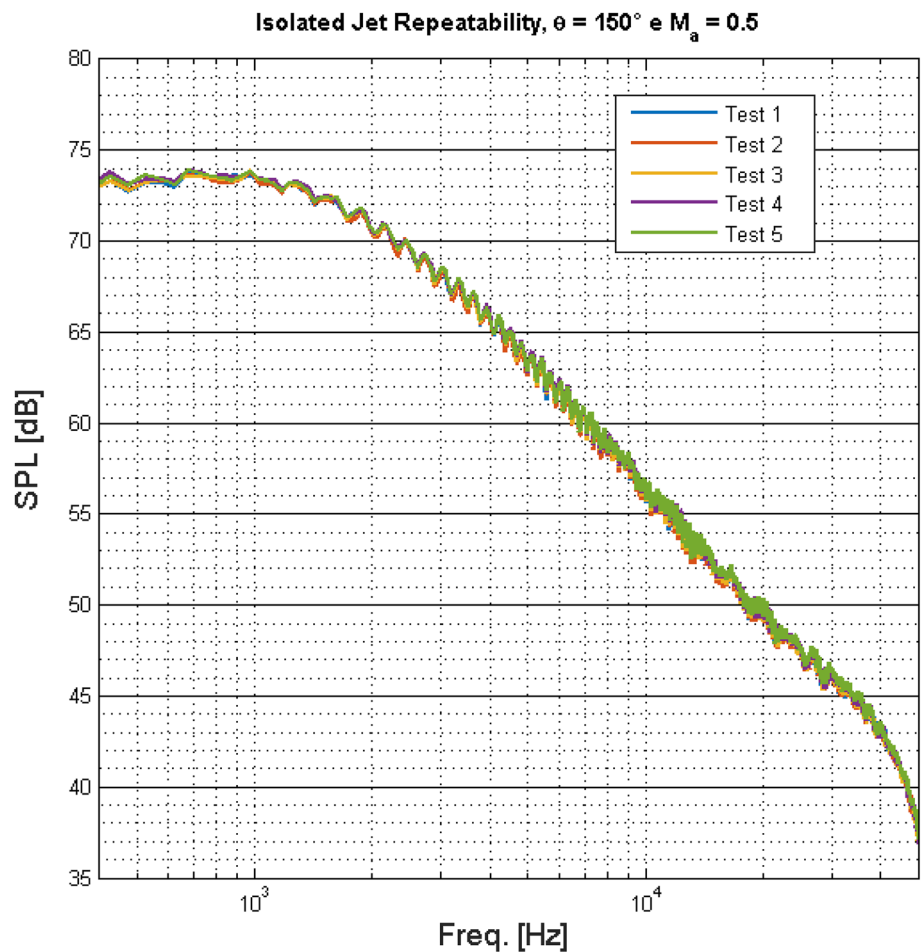
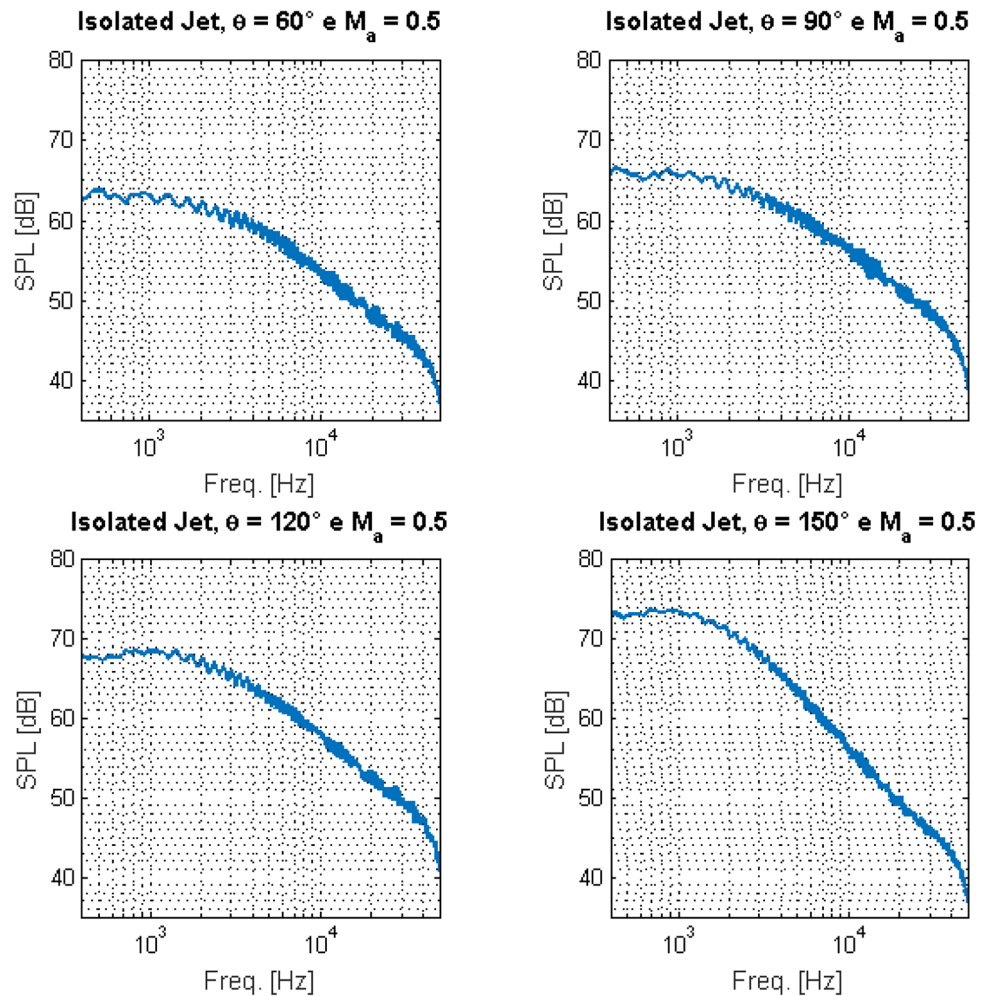


**Fig. 13** Sound pressure level data for different microphone locations ( $60^\circ$ ,  $90^\circ$ ,  $120^\circ$  and  $150^\circ$ ) obtained from 0.5 Mach jets issued by the SMC 000 nozzle. Data obtained at narrowband



atmospheric attenuation function to correct the data due to sound absorption through the atmosphere was used. The farthest position is assumed to be in the far field, and the inverse square law is drawn from that point (blue line). A margin of error ( $\pm 0.5$  dB) is also included (red dashed line) in Fig. 10 as an example. A consecutive alignment of the measured sound pressure levels (SPL) in other positions with the predictions within the error margin is assumed as a sufficient condition to conclude that the measurements are in the far-field region. Otherwise, if there is no consecutive alignment with the last point, even the last position is not accepted as being in the far field.

#### 4 Preliminary evaluations of noise and flow data

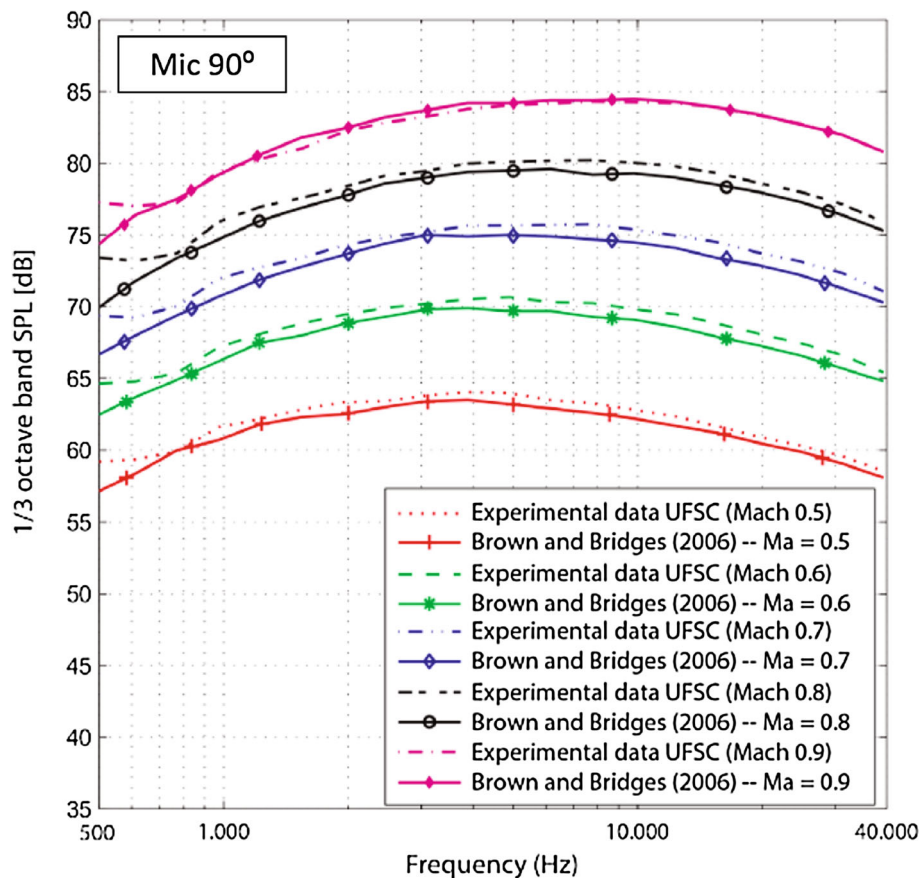
The acoustic field produced by a jet is directly related to its turbulent flow. If this flow is not adequately reproduced in terms of turbulence properties, this can affect the noise data generated [35]. According to Viswanathan [36], differences

of 2–3 dB in the noise data have been reported for different (academic and industrial) facilities from tests with similar operating conditions. The possible causes for these differences are associated with nozzle geometry issues, spurious sound sources upstream the nozzle, Reynolds number effects, test chamber characteristics, etc. [17, 35, 36]. The acoustic and fluid dynamic performance of UFSC's jet rig facility was assessed by comparing measurements of noise and flow velocity with benchmark data available in the literature.

#### 4.1 Velocity and turbulence intensity profiles

According to Bridges and Wernet [37], in a free turbulent jet the most important region concerning aeroacoustic applications is within the first 20 jet diameters. These authors demonstrated through an extensive experimental database that turbulence properties of jet flows over the abovementioned region follow universal scaling laws. These laws were used to evaluate the exit flow conditions as well as to check the turbulent character of the jets

**Fig. 14** Comparisons between the SPL results obtained in the present work and data from Brown and Bridges (2006) [13]. Mach numbers from 0.5 to 0.9 and the nozzle SMC 000



produced at UFSC jet rig by performing hot-wire anemometry measurements at different axial and radial positions along the jet. The results obtained were compared with data from Bridges and Wernet [37] for similar operating conditions and nozzle geometry, namely SMC 000. Figure 11a compares velocity profiles whereas Fig. 11b compares levels of turbulence intensity, both plots obtained for the radial position  $x/D_j = 4$ . Regarding velocity profiles, it can be observed in Fig. 11a that a very good agreement with the literature data is present. However, the levels of turbulence intensity measured were lower than those obtained by Bridges and Wernet [37] (Fig. 11b). These differences can be partly explained because Bridges and Wernet [37] used a boundary layer treatment to physically force a turbulent initial boundary layer and then to obtain higher levels of turbulence intensity. This procedure was not adopted for the flow measurements carried out in the present work. In addition, these differences are to some extent due to the measurement systems employed in the present work (hot-wire anemometry) and by Bridges and Wernet (Particle Image Velocimetry) [37] to obtain turbulence intensity data. It is important to mention that, even though there is a difference between measured and literature data, this does not adversely interfere with the quality of the noise data, as is shown in the next section.

## 4.2 Data repeatability and acoustic cleanliness evaluation

To establish the actual precision of the acoustic data obtained under different weather conditions, a set of jet operating conditions have been used during distinct test campaigns. These tests were conducted over the last 3 years using the SMC000 nozzle. Acoustic data of five different test campaigns are presented in Fig. 12, at narrowband and correspond to 0.5 Mach jets (Fig. 12) issued by the SMC 000 nozzle. Based on results, one can observe that the sound levels repeat within 0.5 dB at the 150° microphone locations throughout the frequency range.

In addition, to evaluate the acoustic cleanliness of UFSC's jet rig facility, sound pressure level data at narrowband, obtained for the 60°, 90°, 120° and 150° microphone locations, are presented in Fig. 13. As can be noted, clean jet noise data are obtained at mentioned locations and over all frequencies.

## 4.3 SPL and OASPL spectra

To evaluate the noise data quality, results of sound pressure level (SPL) in one-third octave band spectra and overall sound pressure level (OASPL) obtained for nozzle SMC

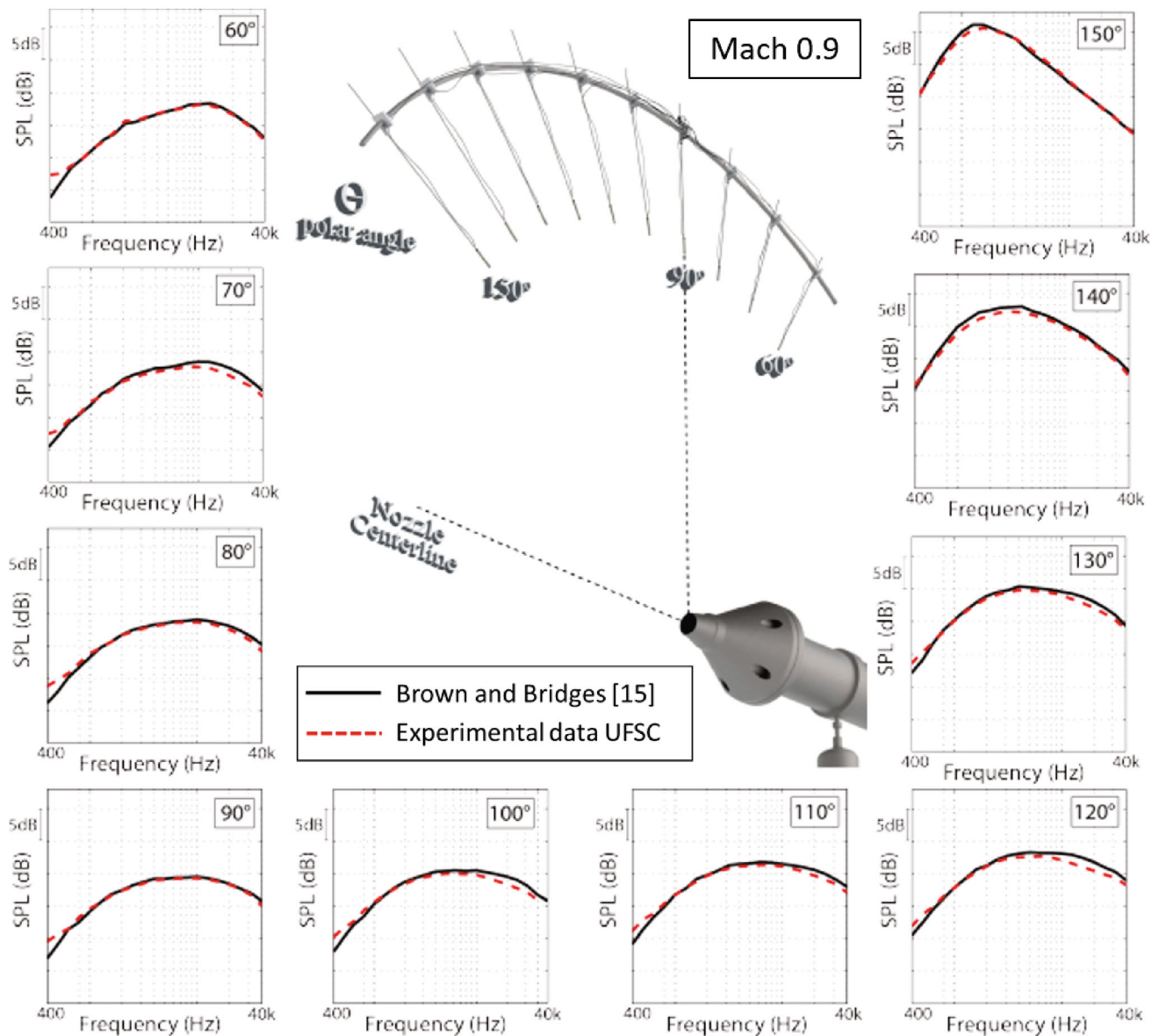


**Fig. 15** Comparisons between SPL results from the present work and data from Brown and Bridges [13] for observer locations from  $60^\circ$  to  $150^\circ$ , using a 0.9 Mach jet and the nozzle SMC 000

000 were compared with data published by Brown and Bridges [13] for the same polar angles, operating conditions and nozzle geometry. In the present work, noise data were obtained with the microphones positioned at a distance of  $44D_j$  ( $\sim 2.23$  m) from the nozzle exit and scaled to  $100D_j$  without applying correction for atmospheric attenuation. In addition, the frequency range used was from 500 Hz to 40 kHz in one-third octave bands using 8-s measuring windows. All measurements were conducted with the microphones set at normal incidence and without the protective grids since they interfere with the frequency response of microphones for very high frequencies (above 20 kHz) and affect the noise results [16, 36].

Figures 14 and 15 show the SPL results corresponding to the microphone positioned at  $90^\circ$  at Mach numbers from 0.5 to 0.9 (Fig. 14), and for observer locations from  $60^\circ$  to  $150^\circ$  for a Mach 0.9 jet (Fig. 15). As can be seen in Figs. 14 and 15, the noise data obtained in this work agree very well with results from Brown and Bridges [13], having differences around 1 dB throughout the frequency range for most spectra. Likewise, good agreement is also observed for the OASPL data obtained for the polar angles from  $60^\circ$  to  $150^\circ$  (Fig. 16) when compared with the data from Brown and Bridges [13]. Figures 17 and 18 show results similar to those shown in Figs. 15 and 16, but with the difference that the acoustic data correspond to a jet with Mach 0.5. According to Figs. 16 and 18, differences within

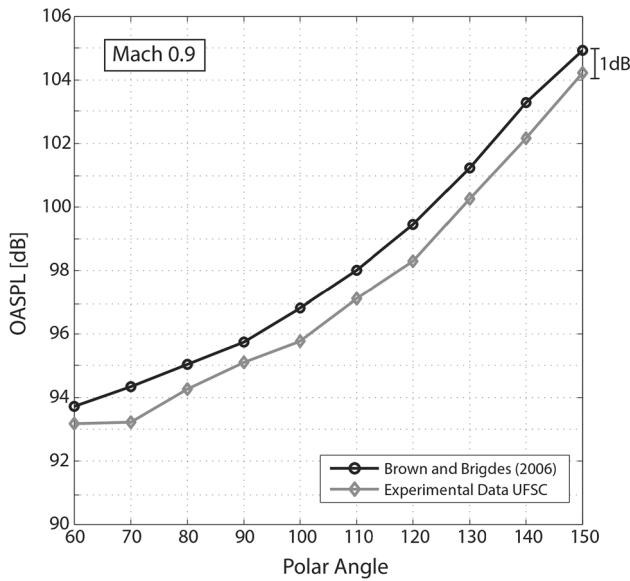


**Fig. 16** Comparisons between OASPL results obtained in the present work and data from Brown and Bridges [13]. Mach 0.9 jet and the nozzle SMC 000

1 dB for OASPL results are observed for most of the observer locations for the jet flows operated at Mach numbers of 0.5 and 0.9. It must be emphasized the fact that data obtained at different facilities would hardly match perfectly due to variability intrinsic to each test environment, involving boundary conditions, instrumentation, operating and ambient conditions, and so on, as also pointed out by Bridges et al. [38].

Other important acoustic considerations about the facility (such as repeatability of additional acoustic data and useful frequency range determination) were outlined in more detail in Siroto et al. [39].

#### 4.4 Power law

Increases in the overall sound pressure level (OASPL) in regard to flow velocity have an analytical prediction through Lighthill’s eight power law. Figure 19a shows the increase in OASPL with flow velocity for angular positions of 60°, 90°, 120° and 150°, while Fig. 19b shows the slope for different angular position measurements. It is valid to stress that these coefficients are based on 1/3 octave band data with a frequency range from 500 Hz to 40 kHz, and results from [13] for the same frequency range are also shown.

Differences in the slope for sound pressure levels were noticed upstream and downstream of the air jet, with downstream OASPL being comparatively higher than those upstream [40–42]. The same behavior is observed in the data acquired at the UFSC jet rig, as seen in Fig. 19a, b. The angular coefficients show a close tendency to the eight-power law up until angular position 120°, from then on the data start to greatly diverge and approach a coefficient close to nine for angular position 150°.

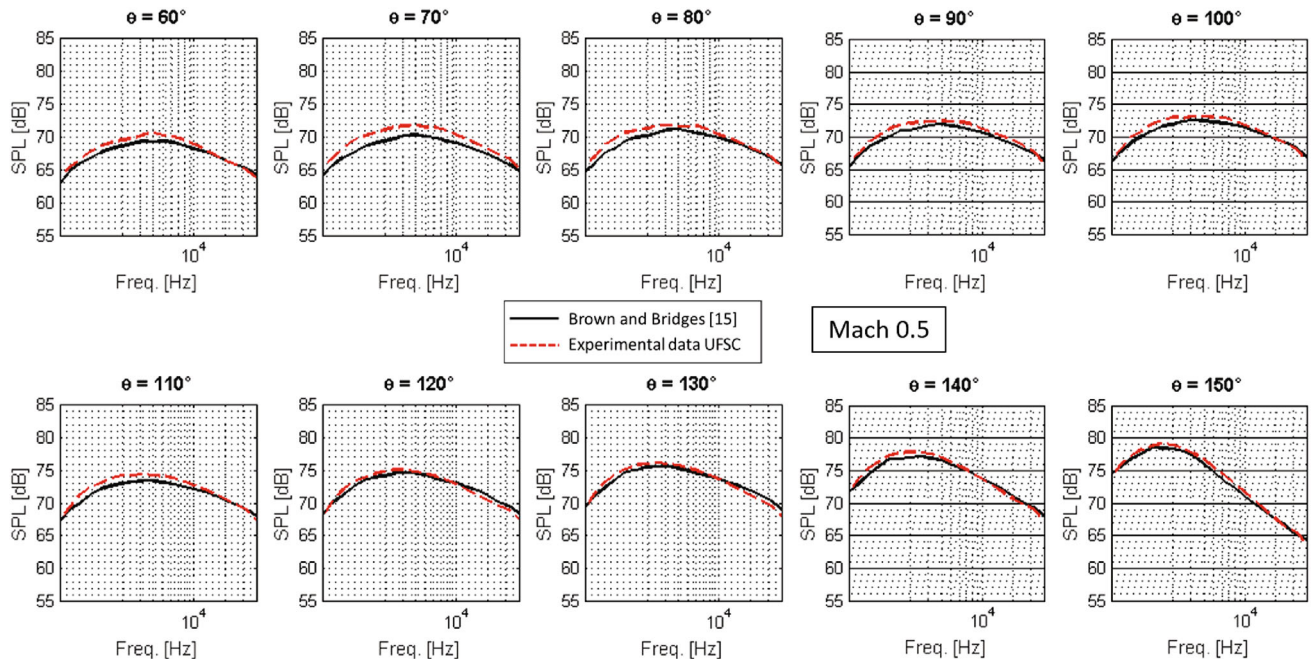


**Fig. 17** Comparisons between SPL results from the present work and data from Brown and Bridges [13] for observer locations from 60° to 150°, using a 0.5 Mach jet and the nozzle SMC 000

**Fig. 18** Comparisons between OASPL results obtained in the present work and data from Brown and Bridges [13]. Mach 0.5 jet and the nozzle SMC 000

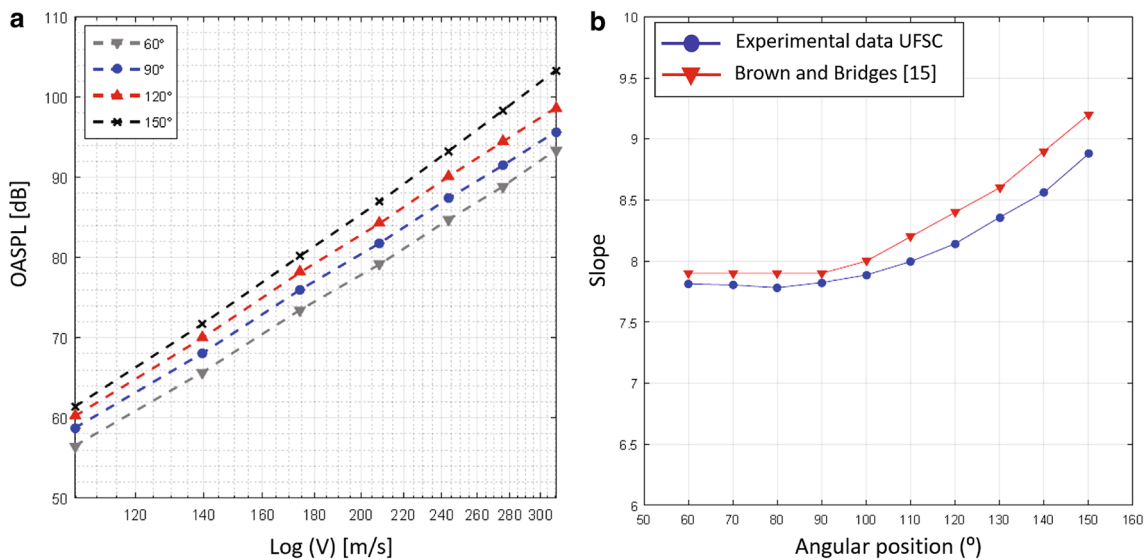
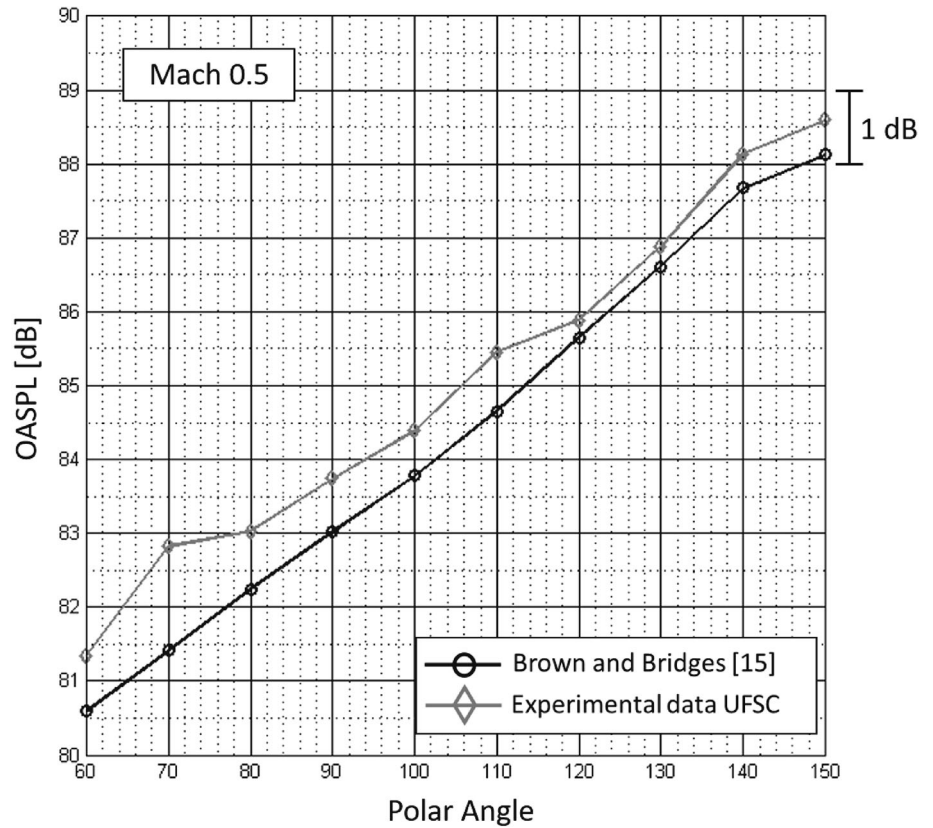


**Fig. 19** **a** Increase in OASPL with flow velocity and **b** angular coefficient for each angular position

### 5 Initial researches on isolated jets and undergoing investigations on installation effects

Initial tests were performed to better understand the main differences on both acoustic and flow fields from isolated jets issued by nozzles SMC 000 and SMC 006. Chevrons

are known to induce streamwise vorticity in the shear layer, which leads to enhanced mixing and reduced potential core length [33, 43]. This is accompanied by the shifting of the acoustic energy of the flow noise sources [44], from low (commonly associated with large-scale structures in the flow) to high (usually attributed to small-scale turbulent structures) frequencies [33].

**Fig. 20** Velocity profiles for axial plans from  $1 < x/D_j < 7$  using a Mach 0.5 jet: nozzles **a** SMC 000 and **b** SMC 006

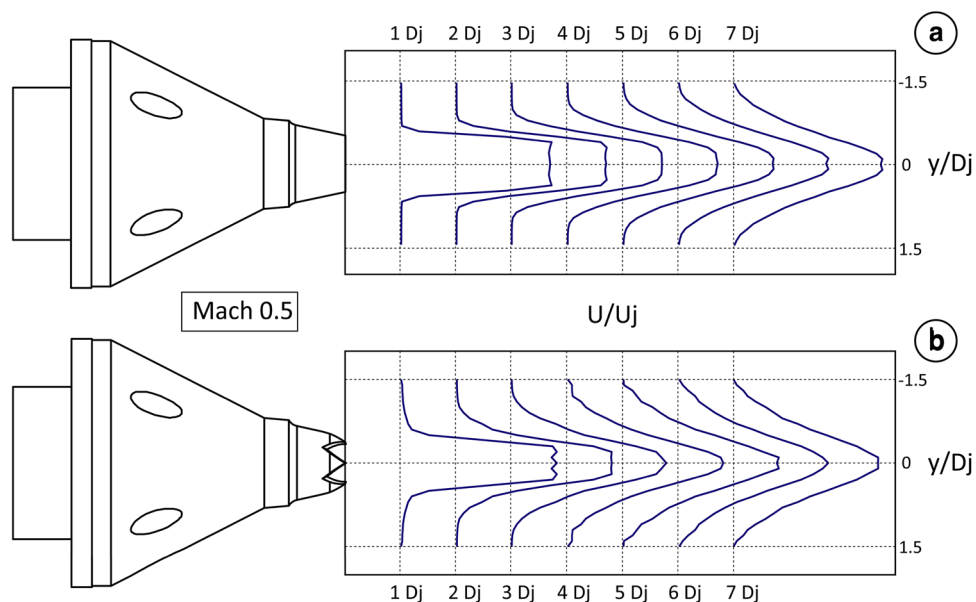
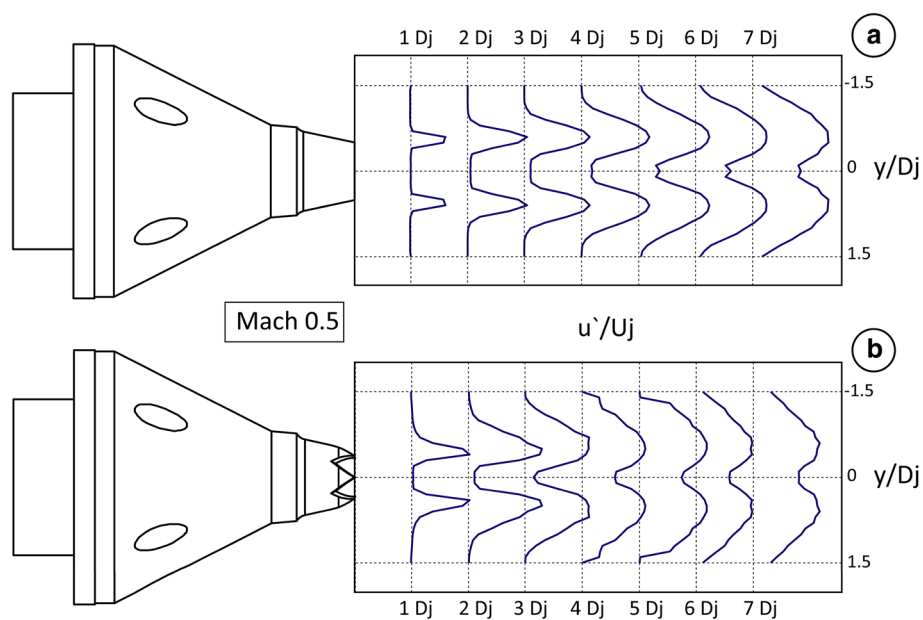


**Fig. 21** Turbulence intensity profiles for axial plans from  $1 < x/D_j < 7$  using a Mach 0.5 jet: nozzles **a** SMC 000 and **b** SMC 006



To emphasize the differences of both the nozzles, baseline (Figs. 20a and 21a) and serrated (Figs. 20b and 21b), Figs. 20 and 21, respectively, compare radial velocity ( $U/U_j$ ) and turbulence intensity ( $u'/U_j$ ) profiles. Flow field data were obtained for axial positions along the jet ( $1 \leq x/D_j \leq 7$ ) by applying hot-wire anemometry technique at Mach 0.5. The flow measurements concerning the chevron nozzle were carried out with the hot-wire probe along a horizontal plane aligned with a valley-to-valley plan. It can be observed from the radial velocity profiles that the serrated nozzle (Fig. 20b) provides smoother velocity gradients than the baseline nozzle (Fig. 20a), indicating higher jet spreading rate and augmented mixing layer, as also

observed by Callender et al. [43]. Regarding the turbulence intensity profiles, one can observe an increase in the peak level associated with the serrated nozzle (Fig. 21b) when compared to that for the baseline nozzle (Fig. 21a), particularly for the first two jet diameters, having an increase of around 38% for  $x/D_j = 1$  and 20% for  $x/D_j = 2$ , once again indicating an augmentation of the mixing layer.

Figure 22 shows PSD results at narrowband, for the microphone location of  $90^\circ$ , as a function of the Strouhal number ( $St = f \cdot D_j/U_j$ ) varying from 0.1 to 11, for both the nozzles operated for Mach numbers from 0.5 to 0.9. As verified by Bridges and Brown [33] and seen in Fig. 22, the chevron nozzle reduces the noise at low frequencies,

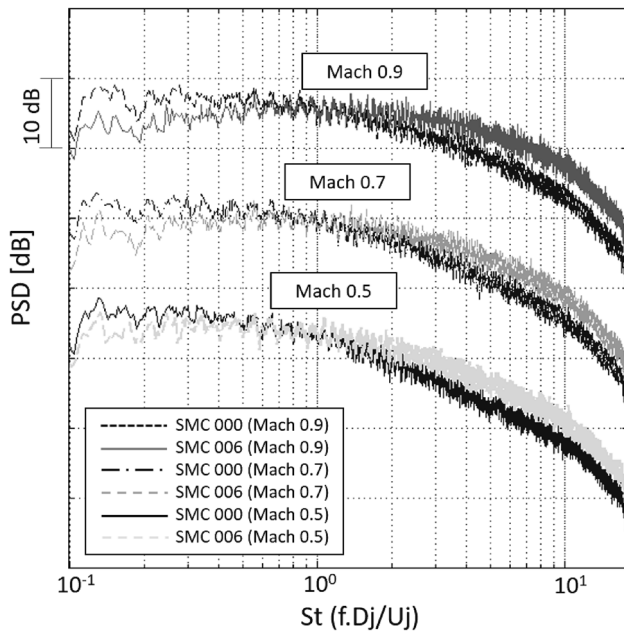


**Fig. 22** PSD results for isolated jets from nozzles SMC 000 and SMC 006 operated from Mach 0.5 to 0.9. Microphone location corresponding to  $90^\circ$

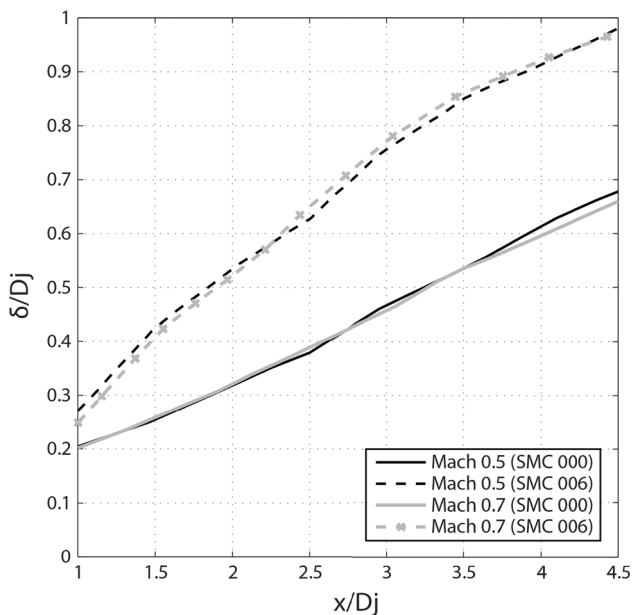


**Fig. 23** Mixing layer thickness for isolated jets from nozzles SMC 000 and SMC 006 operated at Mach 0.5 and Mach 0.7

particularly for  $St < 1$ , and increases noise for  $St > 1$ . This behavior becomes more significant as the Mach number increases, being consistent with the results obtained by Callender et al. [43]. Gutmark et al. [45] observed that chevron nozzles cause significant changes in the flow structure due to the augmented jet spreading, leading to a decrease in the spatial extent of the jet and providing

acoustic reductions. This augmentation of the jet spreading caused by chevrons is also observed according to the mixing layer thickness ( $\delta$ ) values obtained from the hot-wire measurements conducted in the present work (Fig. 23). These flow data correspond to different radial locations along the jets issued from both nozzles for Mach numbers of 0.5 and 0.7. The results in Fig. 23 give another evidence that the mixing layer thickness varies substantially depending on the nozzle geometry and slightly depending on the jet velocity for tests with the same nozzle. As can be seen, the mixing layer thickness of the jet from the nozzle SMC 006 (dashed line) is much thicker than that of the jet from the nozzle.

Currently, the research underway at UFSC jet rig is focused on installation effects on the flow and noise of single cold subsonic jets. In a recent work, experimental investigations were carried out for jets issued by nozzles, with and without chevrons, near a flat plate from jet-overwing mounting configurations, to assess the influence of chevrons on the jet-surface interaction noise and on the shielding effect [30].

## 6 Conclusions and future work

The present work accounted for the development, initial validation and subsequent use of a newly developed jet rig facility at Federal University of Santa Catarina, Brazil, which was initially designed to perform tests with single subsonic cold scaled jets. Major design requirements of a jet rig facility were outlined using the UFSC's jet rig facility as reference. Some difficulties found in the design process were presented and the solutions used to overcome them were discussed. Moreover, the main requirements for test environment to guarantee high-quality noise and flow data were also considered. The procedure adopted for acoustic validation of the anechoic chamber was carried out following the free-field qualification procedure described in the ISO 3745 standard, from which it was found that the cutoff frequency of the chamber is around 400 Hz. Additionally, a complementary procedure was adopted to determine the extension of the far-field region, in the chamber where the inverse square law is valid, by employing the jet as a point source and verifying the corresponding decay of the sound. Based on the results of this test, it was found that  $40D_j$  is the minimal distance from the nozzle centerline for the positioning of the microphones to assure far-field condition. The acoustic and fluid dynamic performance of the facility was assessed by comparing measurements of noise and flow with benchmark data available in the literature for jets issued from a baseline nozzle (SMC 000). The comparisons of results revealed an acoustically clean signature, as well as turbulence

properties in good agreement with data from other facilities. These comparisons indicate that the rig facility is adequate for other investigations involving cold subsonic single jets. Preliminary studies concerning isolated jets issued by serrated (SMC 006) and baseline (SMC 000) nozzles highlighted the main differences observed on the noise and flow fields for different flow conditions. In this regard, the serrated nozzle provided noise reduction at low Strouhal range ( $St < 1$ ) and increased the noise levels at high Strouhal range ( $St > 1$ ) when compared to the baseline nozzle. The UFSC's jet rig is being currently employed to conduct investigations of installation effects. The initial investigations were aimed at assessing the combined effect on acoustic far-field due to different nozzle geometries and vertical distances relative to a flat plate. Future investigations will concentrate on other installation effects related to different nozzle-to-plate configurations, including different nozzle geometries, attached pylon and a flap in different deflection angles.

**Acknowledgements** This study forms part of a joint technical-scientific program of the Federal University of Santa Catarina and EMBRAER. The authors would like to thank Mr. Igor A. Maia for the support to the flow measurements. The financial support from FINEP (Federal Agency of Research and Projects Financing), CNPq (Brazilian Research Council) and CAPES (Coordination for the Improvement of High-Level Personnel) is also acknowledged.

## References

- Casalino D, Diozzi F, Sannino R, Paonessa A (2008) Aircraft noise reduction technologies: a bibliographic review. *Aerosp Sci Technol* 12:1–17. <https://doi.org/10.1016/j.ast.2007.10.004>
- Powell CA, Fields JM (1995) Human response to aircraft noise. In: Hubbard HH (ed) *Aeroacoustics of flight vehicles theory and practice*, vol 2. Noise control. Aeroacoustic Society of America, Woodbury, pp 1–48
- Finkle AL, Poppen JR (1948) Clinical effects of noise and mechanical vibrations of a turbojet engine on man. *J Appl Physiol* 1(3):183–204
- Barbot B, Lavandier C, Chemineé P (2008) Perceptual representation of aircraft sounds. *Appl Acoust* 69:1003–1016. <https://doi.org/10.1016/j.apacoust.2007.07.001>
- Callender WB (2004) An investigation of innovative technologies for reduction of jet noise in medium and high bypass turbofan engines. PhD Dissertation, University of Cincinnati
- Astley RJ (2014) Can technology deliver acceptable levels of aircraft noise? In: *Proceedings of internoise 2014*, Melbourne, Australia
- Campos LMBC (2006) On some recent advances in aeroacoustics. *Int J Acoust Vib* 11:27–45. <https://doi.org/10.20855/ijav.2006.11.1190>
- Omais M et al (2008) Jet noise prediction using RANS CFD input. AIAA Paper 2008-2938
- Karabasov SA et al (2008) Using large eddy simulation within an acoustic analogy approach for jet noise modelling. AIAA Paper 2008-2985
- Ladeinde F et al. (2011) An integrated RANS-PSE-wave packet tool for the prediction of subsonic and supersonic jet noise. AIAA Paper 2011-2704
- Massey SJ et al (2003) Computational and experimental flow field analyses of separate flow chevron nozzles and pylon interaction. AIAA Paper 2003-3212
- Tanna HK, Dean PD, Burrin RH (1976) The generation and radiation of supersonic jet noise, part III, Turbulent mixing noise data. AFAPL-TR-76-65
- Brown C, Bridges J (2006) Small hot jet acoustic rig validation. NASA/TM-214234
- Colonus T, Lele SK (2004) Computational aeroacoustics: progress on nonlinear problems of sound generation. *Prog Aerosp Sci* 40:345–416. <https://doi.org/10.1016/j.paerosci.2004.09.001>
- Dowling AP, Hynes TP (2004) Sound generation by turbulence. *Eur J Mech B Fluids* 23:491–500. <https://doi.org/10.1016/j.euromechflu.2003.10.014>
- Jansson D, Mathew J, Hubner JP, Sheplak M, Cattafesta L (2002) Design and validation of an aeroacoustic anechoic test facility. AIAA Paper 2002-2466
- Tinney CE, Hall A, Glauser MN, Ukeiley LS, Coughlin T (2004) Designing an anechoic chamber for the experimental study of high speed heated jets. AIAA Paper 2004-0010
- Ponton MK, Seiner JM, Ukeiley LS, Jansen BJ (2001) A new anechoic chamber design for testing high-temperature jet flows. AIAA Paper 2001-2190
- Ahuja KK (2003) Designing clean jet noise facilities and making accurate jet noise measurements. AIAA Paper 2003-0706
- Hahn CB (2011) Design and validation of the new jet facility and anechoic chamber. MSc Dissertation, Ohio State University
- Mathew J (2006) Design, fabrication, and characterization of an anechoic wind tunnel facility. PhD Dissertation, University of Florida
- Duell E, Walter J, Arnette S, Yen J (2002) Recent advances in large-scale aeroacoustic wind tunnels. AIAA Paper 2002-2503
- Joslin RD et al (2005) Synergism of flow and noise control technologies. *Prog Aerosp Sci* 41:363–417. <https://doi.org/10.1016/j.paerosci.2005.07.002>
- Martens S (2002) Jet noise reduction technology development at GE aircraft engines. In: 22nd Congress of international council of the aeronautical sciences, UK
- Herkes WH, Olsen RF, Uellenberg S (2006) The quiet technology demonstrator program: flight validation of airplane noise-reduction concepts. AIAA Paper 2006-2720
- Nesbitt E, Mengle VG, Callender B, Czech M, Thomas R (2006) Flight test results for uniquely tailored propulsion-airframe aeroacoustic chevrons: community noise. AIAA Paper 2006-2438
- Bennett GJ et al (2015) Aeroacoustics research in Europe: the CEAS-ASC report on 2013 highlights. *J Sound Vib* 340:39–60. <https://doi.org/10.1016/j.jsv.2014.12.005>
- Detandt Y (2015) Aeroacoustics research in Europe: the CEAS-ASC report on 2014 highlights. *J Sound Vib* 357:107–127. <https://doi.org/10.1016/j.jsv.2015.07.005>
- Saiyed NH, Mikkelsen KL, Bridges JE (2000) Acoustics and thrust of separate-flow exhaust nozzles with mixing devices for high-bypass-ratio engines. NASA TM-209948, Ohio, United States
- Bastos LP (2016) Development and employment of a jet test rig facility for the analysis of installation effects on jets from serrated nozzles. PhD Dissertation, in Portuguese, Federal University of Santa Catarina
- Tam CKW (2004) Computational aeroacoustics: an overview of computational challenges and applications. *Int J Comput Fluid Dyn* 18:547–567. <https://doi.org/10.1080/10618560410001673551>
- Pinker RA (2004) The enhancement of the QinetiQ Noise Test Facility for larger-scale exhaust systems. AIAA Paper 2004-3019
- Bridges J, Brown CA (2004) Parametric testing of chevrons on single flow hot jets. AIAA Paper 2004-2824

34. International Organization for Standardization (ISO) 3745 (2003) Acoustics—determination of sound power levels of noise sources using sound pressure—precision methods for anechoic and hemi-anechoic rooms
35. Zaman KBMQ (2011) Effect of nozzle exit conditions on subsonic jet noise. AIAA Paper 2011-2704
36. Viswanathan K (2003) Jet aeroacoustic testing: issues and implications. AIAA J 41:1674–1689
37. Bridges J, Wernet MP (2010) Establishing consensus turbulence statistics for hot subsonic jets. In: Proceedings of the 16th AIAA/CEAS aeroacoustics conference, Sweden, 2010
38. Bridges J, Brown C, Bozak R (2014) Experiments on exhaust noise of tightly integrated propulsion systems. AIAA Paper 2014-2904
39. Siroto JRLN et al (2016) Validation of cold jet noise rig at Laboratory of Acoustic and Vibration (LVA), Federal University of Santa Catarina (UFSC). In: Proceedings of the 22th international congress on acoustics, Buenos Aires, 2016
40. Khavaran A, Bridges J (2009) Development of jet noise power spectral laws using SHJAR data. AIAA Paper 2009-3378
41. Tam CKW, Viswanathan K, Ahuja KK, Panda J (2008) The sources of jet noise: experimental evidence. J Fluid Mech 615:253–292. <https://doi.org/10.1017/s0022112008003704>
42. Callender B, Gutmark E, Dimicco R (2002) The design and validation of a coaxial nozzle acoustic test facility. AIAA Paper 2002-0369
43. Callender B, Gutmark EJ, Martens S (2010) Flow field characterization of coaxial conical and serrated (chevron) nozzles. Exp Fluids 48:637–649. <https://doi.org/10.1007/s00348-009-0751-1>
44. Nikam SR, Sharma SD (2014) Aero-acoustic characteristics of compressible jets from chevron nozzle. AIAA Paper 2014-2623. <http://dx.doi.org/10.2514/6.2014-2623>
45. Gutmark EJ, Callender B, Martens S (2006) Aeroacoustics of turbulent jets: flow structure, noise sources, and control. Int J Jpn Soc Mech Eng Ser B Fluids Therm Eng 49:1078–1085. <https://doi.org/10.1299/jsmeb.49.1078>